The MCA Method of Determining Thrust of Jet Aircraft in Flight

Richard E. Rosenberg* and Gert Schuch†
German Forces Flight Test Center, Manching, Federal Republic of Germany

From the principle of the conservation of energy, a relationship for thrust is derived, which includes the overall efficiency of the aircraft as a variable. Using this overall efficiency as a key, a technique to determine thrust in flight is developed. In turn, all necessary data are provided for the calculation of the aircraft lift-drag polars.

Nomenclature

C_A = lift coefficient
C_W = drag coefficient
e = specific energy, m
F = component of the resulting thrust vector along the wind direction (propulsive force), N
g = gravitational acceleration, m/s^2
H = geopotential altitude, m
H_u = lower heating value, Nm/kg
Ma = Mach number
m_B = fuel mass, kg
m_F = aircraft mass, kg
n_{za} = load factor along the lift direction
P_H = power consumption of the auxiliary power units, Nm/s
p_s = static ambient pressure, N/m^2
p_n = standard ambient pressure at mean sea level, = 1,013 10^5 N/m^2
S = reference area, m^2
T_s = static ambient temperature, K
T_n = standard ambient temperature at mean sea level, = 288 K
t = time, s
V = true airspeed, m/s
W = component of the resulting aerodynamic force vector in the direction of the relative wind (drag), N
x_g = flight distance along the flight path axis, m
δ = pressure ratio, $=p_s/p_n$
δ_T = throttle setting, %
θ = temperature ratio, $=T_s/T_n$
η = efficiency factor
κ = isentropic exponent

The nomenclature corresponds to German Aerospace Specifications LN 9300 equivalent to ISO specification 1151.

Introduction

IN-FLIGHT verification of lift-drag polars is one of the most important tasks of a flight test department in the assessment of an aircraft design. While lift may be determined relatively easily, drag can only be found indirectly, via the propulsive force acting on the aircraft in the wind axis direction. This propulsive force, aside from the reaction forces produced by the engine, is also dependent upon the aerodynamic forces acting upon the airframe.

Therefore, the most accurate possible measurement of the propulsive force is a key objective of flight testing. The customary methods of measuring propulsive force involve separating the effects of fuselage from those of the engines. This separation is important for performance analysis to further develop the aircraft and is also indispensable for answering warranty questions. However, these methods are not the subject of this paper.

This article describes a procedure based solely on the flight-mechanical dynamics of the total system. With the aid of special flight test maneuvers and a corresponding analysis of selected measurement parameters, it becomes possible to determine the propulsive force—designated here as thrust—as an integral quantity.

The basic idea of this procedure, to which the name MCA method has been given, can, to the best of the authors' knowledge, be traced back to Casetti.[1] MCA stands for Mass Consumption Acceleration and characterizes the elementary physics on which this method is built. The German Forces Flight Test Center took up this idea and, through several years of endeavor, brought the method to the point described in this paper. The procedure turns out to be very simple. However, the analysis has to be tailored to the limitations of flight test, which creates some difficulties in data reduction. In order to identify the problems and eventually to arrive at the solutions described in this paper, flight tests with a series of different types of aircraft, such as G-91, F-104 G, F-4F, Alpha Jet, and Tornado, were necessary. Intermediate results of these efforts have been reported in various internal technical reports. The method was first officially published in its entirety by the authors.[2]

I. Theoretical Relationship

The MCA method is based on the principle of conservation of energy. In particular, it rests upon the conversion of thermal (i.e., fuel) energy into mechanical (potential and kinetic) energy.

Change of Mechanical Energy by External Forces

The change of mechanical energy can be set equal to the work done by the forces acting externally upon the aircraft within a given unit of time.

This change can be generally expressed by the relation

$$m_F g\left(\frac{dH}{dt}+\frac{V}{g}\frac{dV}{dt}\right)=\frac{(F-W)dx_g}{dt} \tag{1}$$

Received Oct. 24, 1984; revision received April 20, 1985. Copyright © 1985 by R. E. Rosenberg. Published by the American Institute of Aeronautics and Astronautics, Inc. with permission.

*Head, Aerodynamics and Flight Mechanics Section, Federal Office of Military Technology and Procurement.

†Aerospace Engineer, Performance Branch, Aerodynamics and Flight Mechanics Section, Federal Office of Military Technology and Procurement.

The expression

$$\frac{dH}{dt}+\frac{V}{g}\frac{dV}{dt}=\dot{e} \tag{2}$$

on the left-hand side of the equation represents the change of the specific energy with respect to time. The difference resulting from thrust and drag on the right-hand side of Eq. (1) is the resulting force doing the work along the flight path coordinate. The time rate of change of flight path distance is the true airspeed, giving

$$m_F g\dot{e}=(F-W)V \tag{3}$$

The definition of F is illustrated in Fig. 1, where the propulsive force can be seen, as a function of standard gross thrust, exit jet interference drag, spillage drag, standard intake drag, and angle of attack α; σ equals the fixed angle of incidence between the exit jet line and the aircraft longitudinal axis. All four force increments are engine installation-related and functions of throttle setting. Therefore, the propulsive force F is also a function of throttle setting.

The drag force W will contain trim drag as a function of control surface deflection required for trim at a given power setting and aircraft center of gravity, which follows from the force balance along the wind direction as given in Eq. (3).

Therefore, the throttle setting plays an important role during the conducting of tests and is treated with special attention in the later section of this article.

Relationship Between Thermal and Mechanical Energy

The fuel energy fed to the aircraft engine in a time unit is transformed into kinetic, potential, and mechanical energy. One must distinguish between the propulsive performance FV, which the system (aircraft) delivers externally, and the secondary power demands P_H within the system. This secondary power is consumed by various onboard systems like the aircraft electric and hydraulic systems and cockpit ventilation.

An equivalent relationship between fuel energy and thrust can be found if one ratios the sum of the two obtainable performance quantities to the required time rate change of fuel energy. In practical terms, this relationship amounts to defining an efficiency factor

$$\eta=(FV+P_H)/\dot{m}_B H_u \tag{4}$$

Relationship to the Thrust

To develop the relation between thermal and mechanical energy, Eqs. (3) and (4) can be combined

$$\eta\dot{m}_B H_u=m_F g\dot{e}+WV+P_H \tag{5}$$

The rate of change of useful thermal energy is expressed by the quantity $\eta\dot{m}_B H_u$, and the rate of change of mechanical energy by the quantity $\dot{e}$ which, according to Eq. (3), depends on the thrust. To determine thrust, one is thus interested in how to transform one form of energy into another; this mechanism can be seen through the differentiation of Eq. (5).

It is advisable to apply the following considerations only for data points having the same values for aircraft mass, drag, and airspeed, respectively. Under these constraints, m_F, W, and V can be set constant in Eq. (5), and differentiation gives a simple relationship between $\dot{e}$, η, and $\dot{m}_B$. The quantity $\dot{e}$, as Eq. (3) shows, varies only with thrust. In Eq. (5) P_H can be set constant without concern inasmuch as experience has shown that in-flight power consumption of the auxiliary power units remains nearly constant. Under these assumptions we gain

$$\frac{d\eta}{d\dot{m}_B}\dot{m}_B+\eta=\frac{m_{F_g}}{H_u}\frac{d\dot{e}}{d\dot{m}_B} \tag{6}$$

As Eq. (2) makes clear, $\dot{e}$ represents the acceleration and climb capacity of the aircraft at a given airspeed. In principle, Eq. (6) shows only the change of this capability along a series of operational points at the same aircraft mass, the same drag, and the same airspeed, as a function of the fuel flow $\dot{m}_B$.

The variable η in Eq. (6) can be replaced by Eq. (4), thus introducing the variable F. In doing so, a direct relation for the thrust from the energy exchange is obtained.

$$F=\frac{1}{V}\left(m_F g\dot{m}_B\frac{d\dot{e}}{d\dot{m}_B}-H_u\dot{m}_B^2\frac{d\eta}{d\dot{m}_B}-P_H\right) \tag{7}$$

The quantities m_F, $\dot{m}_B$, $\dot{e}$, V, and P_H are readily measured in flight. If $d_\eta/d\dot{m}_B$ can be determined, Eq. (7) can be used to calculate thrust. Knowledge of $d\eta/d\dot{m}_B$ is thus the key for in-flight thrust determination and the easiest solution of Eq. (7) would be that for the case $d\eta/d\dot{m}_B=0$.

The following derivations indicate that thrust determination would be practically solved if it were possible to find the operating points, where $d\eta/d\dot{m}_B$ disappears. Returning to Eq. (3) and holding m_F, W, and V constant, we differentiate to show the correlation between F and $\dot{e}$. In incremental form we obtain

$$(m_F g/V)\Delta\dot{e}=\Delta F \tag{8}$$

Thus, the change of $\dot{e}$ between any two operating points "a" and "b" (the same mass, same drag, and same airspeed are still presumed) can be directly expressed as a function of the change of thrust through the relation

$$(m_F g/V)(\dot{e}_a-\dot{e}_b)=F_a-F_b \tag{9}$$

This result says: If the timewise change of the specific energy $\dot{e}_a$ and the thrust F_a at an operating point "a" is known, then the thrust can be determined for any other point "b", provided that $\dot{e}_b$ is known.

The reference values of $\dot{e}$ and F are marked with the subscript R (reference), while the values for the upper limit are written without an index. Thus, a second relation for thrust is obtained, paralleling Eq. (7).

$$F=(m_F g/V)(\dot{e}-\dot{e}_R)+F_R \tag{10}$$

The thrust determined by Eq. (7) can be interpreted as the reference thrust F_R. For the special case $d\eta/d\dot{m}_B=0$, Eq. (7) can be described by

$$F_R=\frac{m_F g}{V}(\dot{m}_B)_R\left(\frac{d\dot{e}}{d\dot{m}_B}\right)_R-\frac{P_H}{V} \tag{11}$$

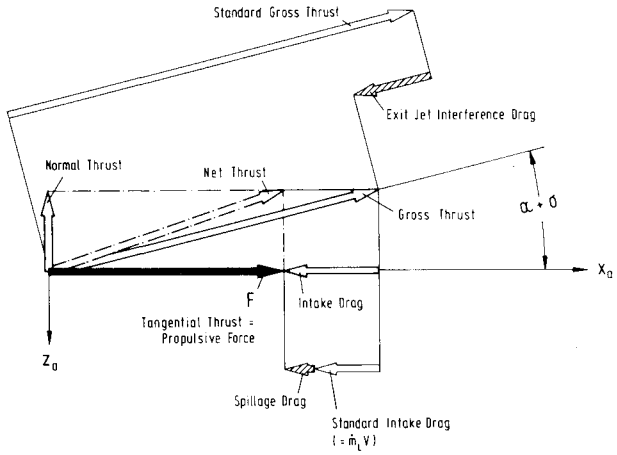

Fig. 1 Force increments, forming the propulsive force F.

where $(\dot{m}_B)_R$ designates the fuel flow at the reference point and $(d\dot{e}/d\dot{m}_B)_R$ the change of the climb and acceleration capacity $\dot{e}$ as a function of the fuel flow. Equation (7) is characterized by the fact that it contains only variables that can be measured in flight. The paired values $\dot{e}_R$, F_R can be inserted in Eq. (10) in order to calculate the required function $F=f(\dot{e})$.

One must, however, be certain that Eqs. (10) and (11) will only be applied to those points of operation, where neither the aircraft mass, drag, nor airspeed change. In this context it should be remembered that the condition m_F, W, V=constant—as a boundary condition for the differentiation of Eqs. (3) and (5)—is a fundamental assumption for the validity of Eqs. (10) and (11).

The objective of the following development is the determination of the reference point, where $d\eta/d\dot{m}_B$ goes to zero in order to determine the paired values $\dot{e}$, F_R.

II Test Sequence

The test sequence is defined by the interrelationship of Eqs. (10) and (11). What is sought is the functional relationship $\dot{e}=f(\dot{m}_B)$ that satisfies these two equations. The test data must be based on the same mass, drag, and airspeed since the boundary conditions m_F, W, V=constant have been used for the differentiation of Eqs. (10) and (11). This requirement leads to a test procedure of wings level ($n_z=1$) accelerations and decelerations at constant altitude (p_s, T_s=constant) over the speed range of the aircraft, each flown at different power settings (δ_T=constant).

The reader should not be confused by the fact that the quantities m_F, W, and V are subject to continuous changes (contrary to the emphasis of the boundary conditions m_F, W, V=constant). The crucial point of this test sequence is that for each selected power setting (δ_T=constant), the speed range and thus the drag envelope of the aircraft will be covered. The desired boundary conditions of m_F, W, and V=constant are obtained by analysis that appropriately cross-plots the test data. For this purpose, the test data $\dot{e}=f(\dot{m}_B)$ are collected at constant airspeeds V and corrected to a mean reference mass m_F with common flight test procedures, i.e., as given in Ref. 3. In stabilized horizontal flight (with p_s and T_s assumed to be constant) the drag is only dependent on airspeed. If the aircraft is accelerated, as suggested above, the drag depends also on dV/dt according to Eqs. (3) and (2). However, flight test results have proved that the influence of acceleration on drag can be ignored. Therefore, the condition W=constant is also satisfied along with the condition V=constant for horizontal flight points. This test procedure is shown schematically in Fig. 2 for an altitude H and three different power settings δ_T. This test method produces a large range of measured values for $\dot{e}=f(\dot{m}_B)$. This result is related to the known behavior of the kidney-shaped curves of $\dot{e}$, which collapse together with ever-decreasing power settings.

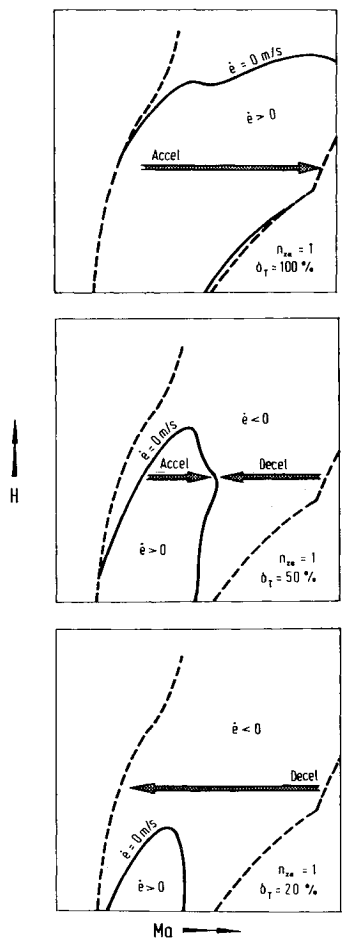

Fig. 2 Accelerations and decelerations performed at different power settings.

III. Test Evaluation

Fairing of the Measurements

Choose m_F, p_s, T_s, and δ_T as parameters, and plot $\dot{e}$ and $\dot{m}_B$ as functions of V (see Figs. 3 and 4).

The transition from the nonstationary ($\dot{e}\neq 0$) to the stationary flight state ($\dot{e}=0$, see also Fig. 2) is asymptotic; therefore, the maneuvres, in the example shown, have been aborted prematurely in order to save flight time. For this reason, the parameter curves δ_T=constant do not go to the corresponding end values (gaps occurring at $\dot{e}=0$). Even so, the airspeeds for any given δ_T= constant can be read from Fig. 3 very reliably at the intersection of the curve extrapolations to the axis $\dot{e}=0$. The corresponding fuel flow values can be found by an extrapolation of the corresponding curves in Fig. 4. The plotted measurements have been corrected with the aid of commonly used flight test techniques[3] to a normalized weight, constant center of gravity, and constant altitude.

Figure 5 is a result of cross-plotting and represents the foundation for further analysis inasmuch as the conditions m_F=constant and W=constant are satisfied along the parameter curves V=constant. In this graph the reference points are sought where the quotient $d\eta/d\dot{m}_B$ goes to zero.

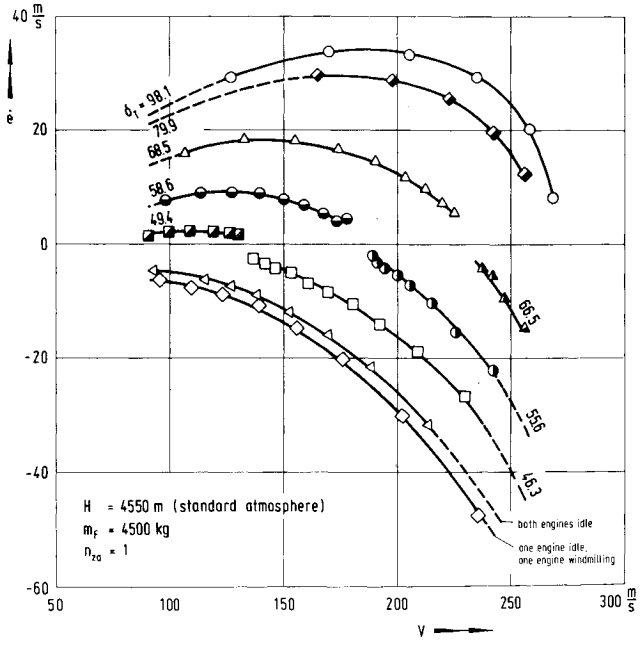

Fig. 3 Course measured $\dot{e}=f(V)$ (twin jet combat aircraft).

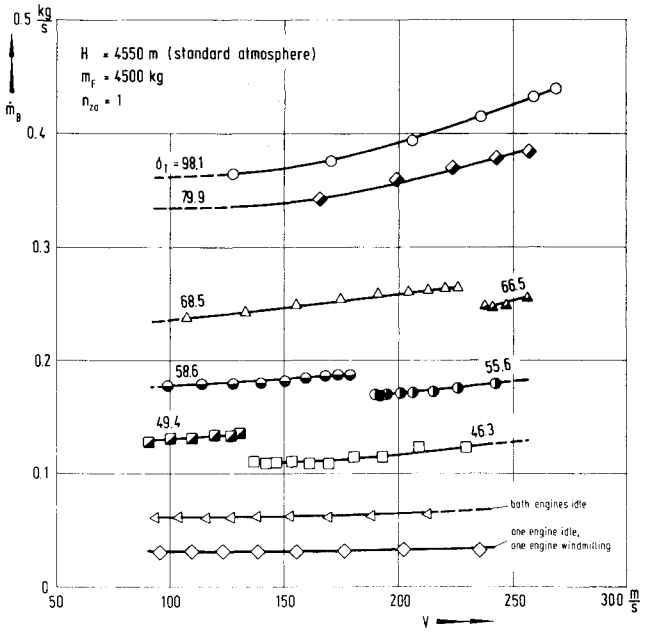

Fig. 4 Course measured $\dot{m}_B = f(V)$ (twin jet combat aircraft).

The symbols correspond to the symbols that mark the different power settings δ_T in Figs. 3 and 4.

Determination of the Reference Point

The determination of the reference point requires careful analysis. For example, the arbitrarily selected curve of $V = 135$ m/s was chosen from Fig. 5 and is redrawn in Fig. 6.

The curve V = constant (see Fig. 6a) has arbitrary reference points; R_1 corresponds to the idle operating point and R_n to the military operating point of the engine in the nonafterburning thrust region. The afterburning thrust region must be specially handled since it represents a fundamentally different operational relationship from that of nonafterburning operation. In practical terms, it corresponds to another kind of aircraft. Flight test data would, as a result, yield a different kind of functional relationship for $\dot{e} = (\dot{m}_B)$ for a given V = constant with afterburner operation.

Assuming $\mathrm{d}\eta/\mathrm{d}\dot{m}_B = 0$, a fictitious efficiency curve r is determined for each of these individual reference points with the help of

$$\eta = \frac{m_F g}{\dot{m}_B H_u}\left[\dot{e} - \dot{e}_R + (\dot{m}_B)_R \left(\frac{\mathrm{d}\dot{e}}{\mathrm{d}\dot{m}_B}\right)_R\right] \tag{12}$$

Equation (12) is derived from the combination of Eqs. (11), (10), and (4). One observes that P_H/V vanishes. The extreme values of the family of curves r which follow the dot-dash line in Fig. 6a correspond to the reference points R, where $\mathrm{d}\eta/\mathrm{d}\dot{m}_B$ has been initially set equal to zero. Further evaluation is necessary to find the actual efficiency factor from the family of curves.

The efficiency factor curves between $(\dot{m}_B)_{Rn}$ and $(\dot{m}_B)_{R1}$ elicit the following observations: The curve r_n, which corresponds with R_n, tends toward negative values for $\dot{m}_B \to 0$. If R converges to R', the curve r moves to higher efficiency factor values (toward the upper left corner in Fig. 6b) and tends to approach the limit curve r' as its maximum moves along the dot-dash line. Especially in the idle thrust range at $(\dot{m}_B)_{R1}$, the slopes of the curves are drastically changed. They clearly turn up from negative to positive values of the efficiency factor.

If R exceeds R' (Fig. 6a), the corresponding curve r falls below the limit curve r'. Because the curve V = constant has no measurements below R_1, r_1 is the last obtainable set of efficiency factors that can be determined by this method; these curves have local minima at $(\dot{m}_B)_{R1}$.

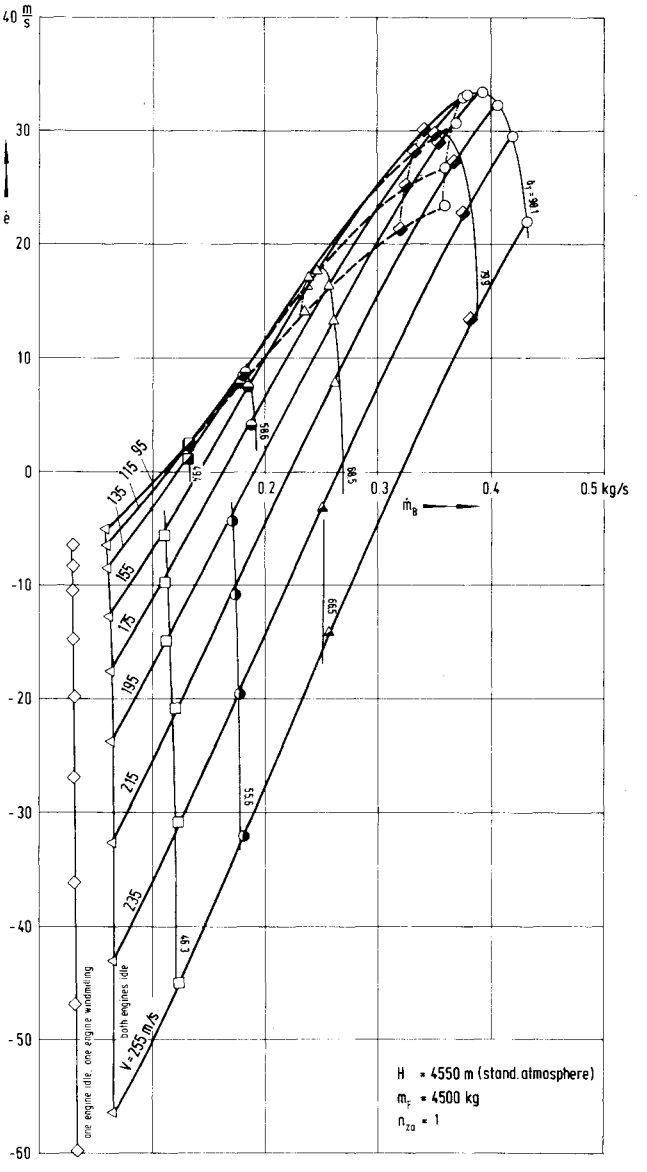

Fig. 5 Function $\dot{e} = f(\dot{m}_B)$, determined using Figs. 3 and 4.

Figure 6b illustrates that the area between $(\dot{m}_B)_{R1}$ and $\dot{m}_B = 0$ determines which efficiency factor curve of the family r is physically realistic. The behavior of the curve at the limit with $\dot{m}_B = 0$ (where the supplied fuel power disappears) is of special importance. As Eq. (12) shows, one and only one efficiency factor curve in the family of r curves of Fig. 6 has a realistic end value η_0 at $\dot{m}_B = 0$. It is the curve designated r^*, corresponding to reference point R^*, whose coordinates $\dot{e}_{R^*}$ and $(\dot{m}_B)_{R^*}$ exactly fulfill the condition

$$\dot{e}_{R0} - \dot{e}_{R^*} + (\dot{m}_B)_{R^*}(\mathrm{d}\dot{e}/\mathrm{d}\dot{m}_B)_{R^*} = 0 \tag{13}$$

Here $\dot{e}_{R0}$ is the rate of change of the specific energy at $\dot{m}_B = 0$ (see also Fig. 6b). Since Eq. (12) results in an indeterminate form, μ_0 cannot be quantified directly. All other efficiency curves clearly tend to $+\infty$ or $-\infty$ at $\dot{m}_B = 0$, which sets the curve r^* apart from the rest of the family of curves as the only realistic set of efficiency factors. Equation (12) also implies that the r^* curve must exhibit a second extreme value (a minimum) at the point R_0 in addition to the maximum value at the point R^*. This result follows from the fact that the in-

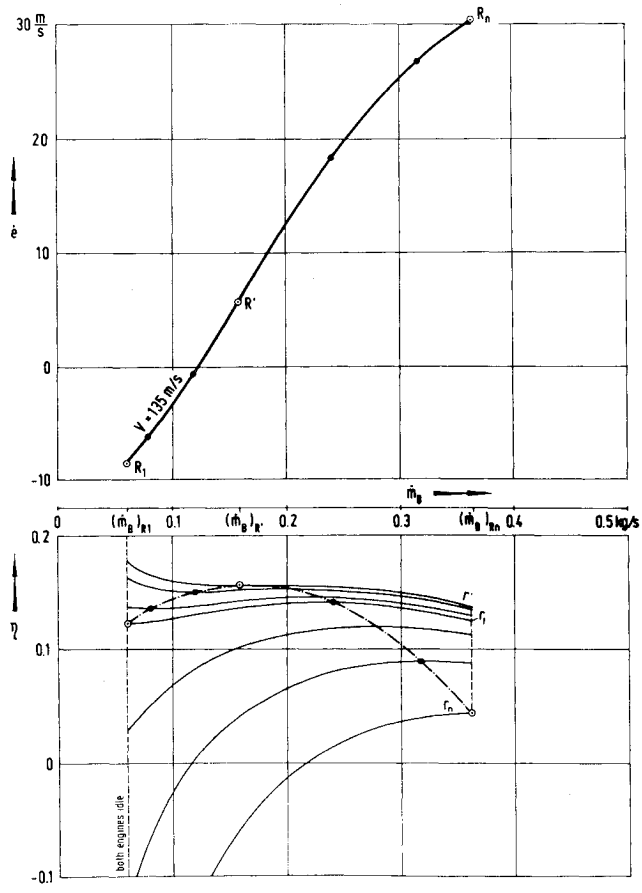

Fig. 6a Determination of the efficiency curve between full-power and two-engine idle point.

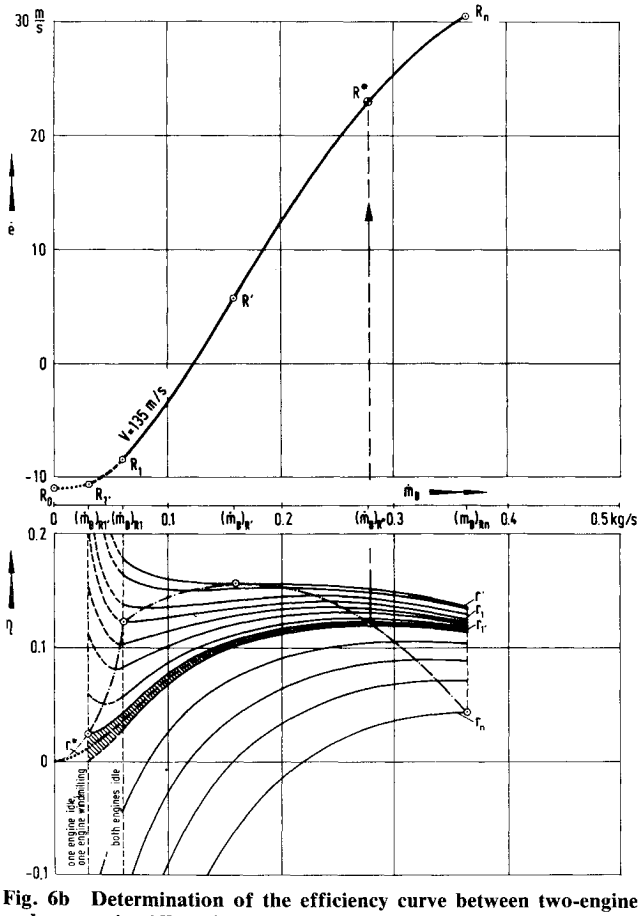

Fig. 6b Determination of the efficiency curve between two-engine and one-engine idle points.

definite expression $\eta_0 = 0/0$ also occurs when $R = R_0$. In order to identify the r^* curve, the individual efficiency factor curves have to be extended into the area around $\dot{m}_B = 0$. This extension can be computed with the help of Eq. (12). The values $\dot{e}$, $\dot{m}_B$ for a constant V must be known in this region.

The end point R_0 of the curve at $\dot{m}_B = 0$ is only attainable with a windmilling engine, a test point that is not practical for high-performance aircraft. The only reasonable approach to extending the curve at constant V in this area is to use the one-engine-at-idle approach. There are no definable operating conditions between the two idle points since control of fuel consumption is no longer possible in the transition region. Therefore, an extrapolation of the curve V = constant must be used. The curve for constant V is extrapolated from R_1 to $R_{1'}$, in Fig. 6b.

Although the fuel flow is almost instantaneously reduced from $(\dot{m}_B)_{R1}$ to $(\dot{m}_B)_{R1'}$, when one engine is shut down, there is no abrupt loss of thrust. Considerable energy (kinetic energy in the rotor, thermal energy in the components) is still stored in the engine. The thrust decays exponentially. To extrapolate, it can be assumed that $\dot{e}$ will continuously decrease between R_1, and $R_{1'}$ (dashed line in Fig. 6b). Using Eq. (12), the efficiency curves calculated as described previously (Fig. 6a) can be traced up to the single-engine idle point $R_{1'}$. The final efficiency curve obtained in this manner is the $r_{1'}$ curve, which has a minimum at $R_{1'}$. With a single-engine aircraft, however, the point R_1 corresponds naturally to the lowest operating point that can be obtained, and the extrapolation to the area around $\dot{m}_B = 0$ has to be done using only this point. However, experience gained with F-104 and G-91 aircraft shows that with a single-engine aircraft this point will probably correspond closely to the point $R_{1'}$ of a multi-engine aircraft.

In practice, a positive as well as a negative value for η_0 is possible for $\dot{m}_B = 0$; this efficiency depends totally on the sign of the net thrust F (i.e., the difference between input and output impulse) in this region, as seen in Eq. (4). Negative thrust in this region is possible because of pressure and velocity fields at the inlet and exit areas with a windmilling rotor (or even with rotors driven by the airflow). At this point, however, the simplified assumption is made that η_0 goes to zero at $\dot{m}_B = 0$. The resulting error in the final results can be neglected, as will be demonstrated later.

The connecting line of the extreme values for r (dot-dash line) is extended to the origin of the coordinates. The desired efficiency factor r^* then lies inside the shaded area in Fig. 6b and logically reaches its minimum at $\dot{m}_B = 0$. The upper boundary for the shaded area is given by the curve r'. The lower boundary is established by the efficiency curve intersecting the abscissa at $(\dot{m}_B)_{R1}$. Both curves are defined by the single-engine idle point, up to which the V = constant curve is measurable.

The coordinates of the efficiency curve r^*, scaled from Fig. 6b, establish the V = constant curve from $R_{1'}$ to R_0, and thus the end point $\dot{e}_{R0}$ is determined by

$$\dot{e} = \frac{H_u}{m_F g} \int \left(\eta + \dot{m}_B \frac{\mathrm{d}\eta}{\mathrm{d}\dot{m}_B} \right) \mathrm{d}\dot{m}_B + C \tag{14}$$

This equation can be solved in a closed numerical form with the aid of the equation

$$\eta = a_0 + a_1 \dot{m}_B + a_2 \dot{m}_B^2 + a_3 \dot{m}_B^3 \tag{15}$$

The values a_0, a_1, a_2, and a_3 are constants (not covered in the nomenclature), which can be determined.

The solution is of the form

$$\dot{e} = (H_u / m_F g) \{ a_0 [\dot{m}_B - (\dot{m}_B)_{R1}] + a_1 [\dot{m}_B^2 - (\dot{m}_B^2)_{R1}] \ldots + a_3 [\dot{m}_B^4 - (\dot{m}_B^4)_{R1}] \} + \dot{e}_{R1} \tag{16}$$

where one evaluates the integration constant with the help of the measured coordinates $\dot{e}_{R1}$, $(\dot{m}_B)_{R1}$ of the two-engines-at-idle point.

Test results indicate that for aircraft with sufficiently separated nozzles (no mutual interaction of the exhaust gas stream) $\dot{e}$ decreases by the same amount along the V = constant curve (expressed by the equation $\dot{e}_{R1} - \dot{e}_{R1'} = \dot{e}_{R1'} - \dot{e}_{R0}$) as each engine is shut down. These results are physically realistic. At least for this category of aircraft, it appears that R_0 can be determined in a very simple way without having to take into account the efficiency. This hypothesis, of course, must be verified by further tests.

The maximum of the efficiency curve r^* occurs where r^* intersects with the dot-dash line interconnecting the extreme values (Fig. 6b). The location of the reference point R^* on the V = constant curve is simultaneously determined.

The point R_0, where the efficiency curve r^* has its minimum, is also of interest. The curve r^* can be thought of as a trend line, showing the behavior of the fictitious efficiency curves in the $\dot{m}_B = 0$ area. Below $r^*$the curves tend toward $-\infty$, above r^* toward $+\infty$. The break in the dot-dash line (connecting the extreme values) shows that, practically, a different set of physical laws governs when the engines are shut down. R_0 is the terminal point of a line tangent to the constant curve at the point R^*, as is easily seen from the bracketed expression in Eq. (12).

Determination of Thrust

After combining Eqs. (10) and (11), the thrust equation with R^* as the reference point can be expressed in the form

$$F = \frac{m_F g}{V}\left[\dot{e} - \dot{e}_{R^*} + (\dot{m}_B)_{R^*}\frac{\mathrm{d}\dot{e}_{R^*}}{\mathrm{d}(\dot{m}_B)_{R^*}}\right] - \frac{P_H}{V} \qquad (17a)$$

When point R_0 is used as a reference point, this equation can be expressed more simply

$$F = (m_F g/V)\,[\dot{e} - \dot{e}_{R0}] - (P_H/V) \qquad (17b)$$

The two reference points R^* and R_0 lead to the same results. The quantity P_H/V is found from the engine manufacturer's documentation or by measurements.

Equation (17) allows calculation of the thrust function $F = f(\dot{m}_B)$ along the V = constant curve. Figure 7 shows the family of curves $F = f(\dot{m}_B, V)$ determined under the test conditions p_s = constant and T_s = constant as described above (Fig. 4 and 5).

Common flight test methods, i.e., as shown in Ref. 3, are used to adjust the thrust to standard day conditions and to reduce the expression to nondimensional form

$$\frac{F}{\delta} = f\left(\frac{\dot{m}}{\delta\sqrt{\theta}},\ Ma\right) \qquad (18)$$

where δ represents the ratio of the static ambient pressure p_s to the reference pressure $p_n = 1{,}013 \cdot 10^5$ N/m^2 and θ the ratio of the static ambient temperature T_s to the reference temperature $T_n = 288$ K (on standard day at mean sea level). This relationship also ties the MCA method to the relevant literature, with Eq. (18) the usual basis for flight performance calculations.

Calculation of Aircraft Drag Polars

The aircraft polar describes, as stated earlier, the interconnection between lift coefficient C_A and the drag coefficient C_w of the aircraft, namely, as a function of the Mach number Ma. Thus, the test sequence described previously provides all data for the calculation of the drag polar related to each reference point found in Fig. 6.

In cruising flight, C_A and C_w are given by

$$C_A = (2m_F g n_{za})/p_s Ma^2 \kappa S) \qquad (19)$$

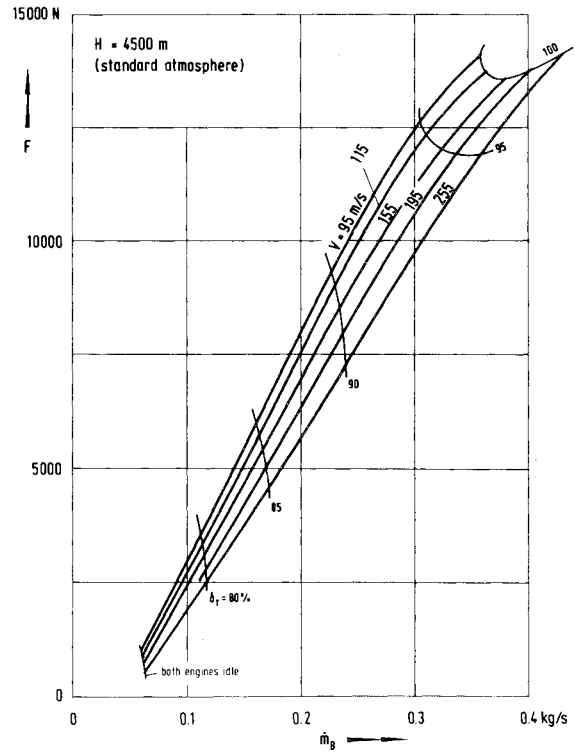

Fig. 7 Thrust characteristics.

and

$$C_w = \frac{2}{p_s Ma^2 \kappa S}\left(F_{R^*} - \frac{m_F g}{Ma\sqrt{\kappa R T_s}}\,\dot{e}_{R^*}\right) \qquad (20)$$

In Eq. (20) F_{R^*} represents the thrust force and $\dot{e}_{R^*}$ the corresponding rate of change of specific energy at the reference point R^* (see Fig. 6). In principle, from the total of all accelerations and decelerations performed at different throttle settings δ_T, plots of C_A and C_w vs Ma can be obtained for each altitude H (see Figs. 8 and 9). Polars can be obtained by cross-plotting between these two sets of curves as shown in Fig. 10.

The data points on the heavy lines in Figs. 8 and 9 correspond to the same example on which Fig. 5 is based. Since these points alone will not define the polars at a given Mach number, the additional points from other test altitudes are also included.

Experience shows that Reynolds number effects have not been significant in the cases examined (no change of polars at higher altitudes). However, if an influence is suspected, the MCA method may be applied separately for the low- and high-altitude regimes.

Because F and W are functions of power setting, those polars derived using the MCA methodology will be strictly configuration-oriented. However, they will be immediately suitable for in-flight performance calculations since trim and engine effects are included.

In Fig. 10 the polars derived using the MCA methodology are compared with the same set of polars gained by conventional methods. As can be seen, both sets of curves are almost identical. They are both root-mean-square fits of the evaluated data points. In both cases, the accuracy of the curve fit finally depends on the accuracy of the flight test instrumentation. Error analysis shows that the scatter of the MCA data is in the order of ± 2 and ± 7% (corresponding to drag counts between 0.5 and 2.0). However, compared to the MCA method, which requires relatively few measurement parameters and a straightforward analysis, the conventional method is very complex, as is generally known. In this case, F

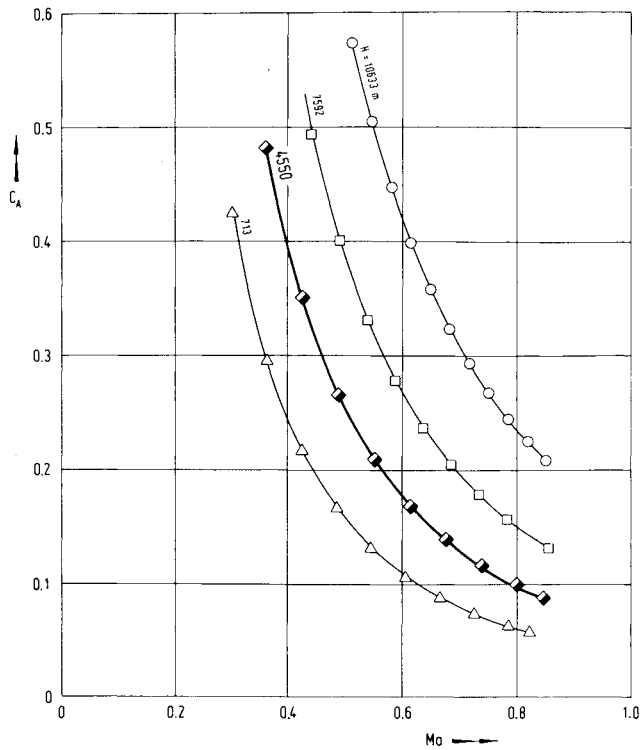

Fig. 8 Functions $C_A = f(Ma)$ obtained at different altitudes.

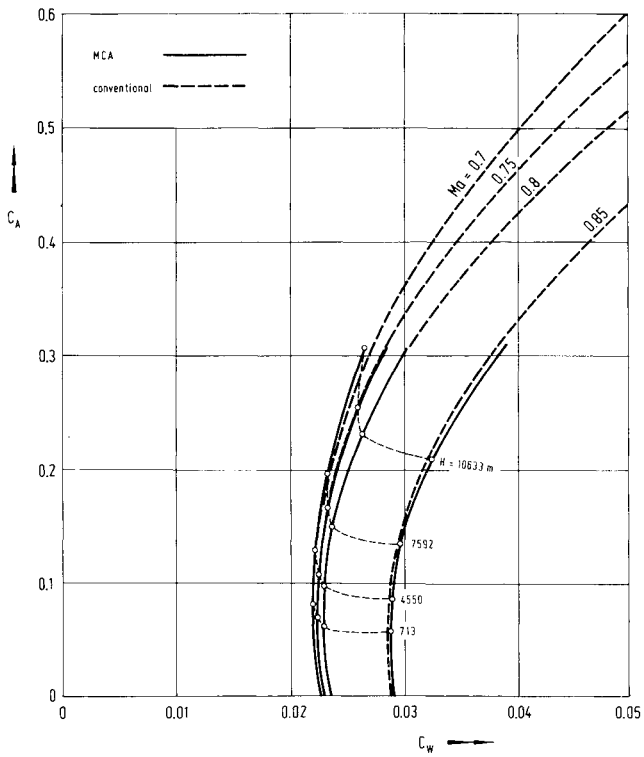

Fig. 10 Aircraft drag polars.

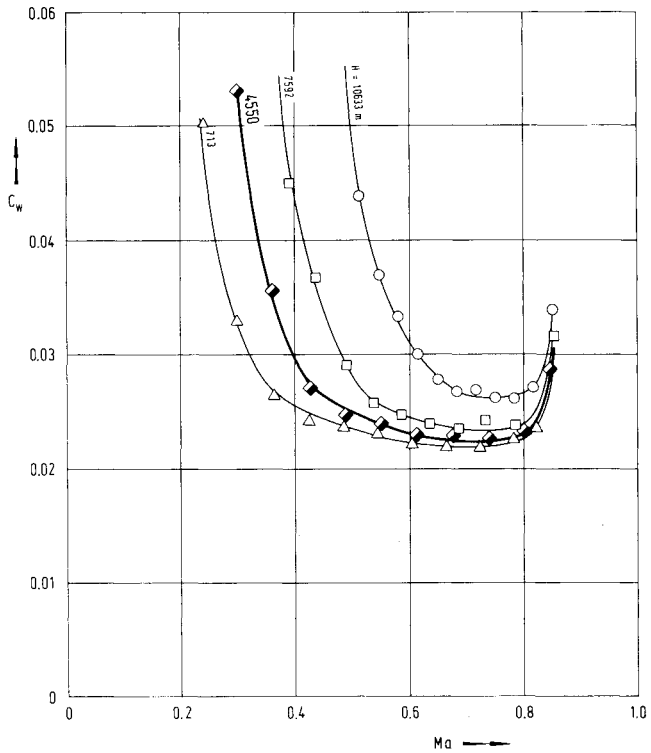

Fig. 9 Functions $C_W = f(Ma)$ obtained at different altitudes.

must be determined by detour, via the force increments, as illustrated in Fig. 1: Standard gross thrust and air mass flow (to determine standard intake drag) are evaluated from correlations against combinations of various parameters, such as pressure, temperature, fuel flow, and shaft speed, which can be measured in flight. These correlations of thrust and airflow against the measured parameters must be determined by full-scale calibration in a ground test facility, where measurements of thrust and airflow are available. To establish the exit jet interference drag as well as the spillage drag, it is essential to carry out wind-tunnel tests at model scale in order to again provide the relationship to parameters, which can be measured in flight. Finally, extensive calculations using very complex computer programs, which model the engine behavior in flight, are required to combine all these data and to determine the propulsive force F.

Conclusion

The advantage of the MCA method is that it requires very few, commonly available measurement parameters: aircraft mass m_F (i.e., takeoff mass m_{F0} and fuel quantity m_B), fuel flow $\dot{m}_B$, change rate of the specific energy $\dot{e}$ (that is accelerations in direction of the three axes along with the angle of incidence), true airspeed V, and the ambient conditions p_s, T_s. Most important, no specially instrumented and calibrated engines are required.

Simplification of the principles for this article should not hide the fact that utilization of this procedure still requires a great deal of detailed work in order to arrive at a reliable result. The details start with the installation and calibration of the aircraft instrumentation (in particular with the accelerometers and flow meters) and continue with the correction and data reduction of the individual measurements all the way to the final output product. The experienced flight test engineer, however, will recognize the individual problem areas, and apply available techniques to overcome the problems. One of the most important considerations is efficient computer programming, since a large amount of data has to be processed. At the same time, a feel for the flight mechanics involved is required; this feel cannot be completely replaced by even the most careful programming.

The MCA method cannot and should not completely replace thrust measurement with calibrated engines. They are still regarded as an important aid for the developing and op-

timizing engine and airframe. However, the method does have the advantage of giving a simplified way of determining the propulsive force. The flight mechanics engineer needs this force to determine the lift-drag polars as well as the aircraft performance.

The MCA method is a simple tool for a test center, which is more interested in the expeditious testing of the flight performance of complete airplanes than in the optimization of the individual airframe and engine components.

References

[1]Casetti, M., "Method for Thrust Measuring the Engine Thrust, the Aerodynamic Coefficients and the Performance of an Aircraft through Flight Testing," Working Paper to Tornado Management Organization, Dec. 1972.

[2]Rosenberg, R. and Schuch, G., "Die M.C.A.-Methode ein flugversuchstechnisches Verfahren zur Ermittlung des Schubes von Strahlflugzeugen Fluge," *Zeitschrift für Flugwissenschaften und Weltraumforschung*, Vol. 6, 1982, pp. 383.

[3]*AGARD Flight Test Manual*, Pergamon Press, New York, 1962.

The news you've been waiting for...

Off the ground in January 1985...

Journal of Propulsion and Power

Editor-in-Chief
Gordon C. Oates
University of Washington

Vol. 1 (6 issues) 1985 ISSN 0748-4658
Approx. 96 pp./issue
Subscription rate: $170 ($174 for.)
AIAA members: $24 ($27 for.)

To order or to request a sample copy, write directly to AIAA, Marketing Department J, 1633 Broadway, New York, NY 10019. Subscription rate includes shipping.

"This journal indeed comes at the right time to foster new developments and technical interests across a broad front." —**E. Tom Curran,**
Chief Scientist, Air Force Aero-Propulsion Laboratory

Created in response to *your* professional demands for a **comprehensive, central publication** for current information on aerospace propulsion and power, this new bimonthly journal will publish **original articles** on advances in research and applications of the science and technology in the field.
Each issue will cover such critical topics as:

- Combustion and combustion processes, including erosive burning, spray combustion, diffusion and premixed flames, turbulent combustion, and combustion instability
- Airbreathing propulsion and fuels
- Rocket propulsion and propellants
- Power generation and conversion for aerospace vehicles
- Electric and laser propulsion
- CAD/CAM applied to propulsion devices and systems
- Propulsion test facilities
- Design, development and operation of liquid, solid and hybrid rockets and their components